tistically insignificant. Attenuation measurements are still in progress, and results on the remaining three fibers will be presented at IOOC81.

Bandwidth was measured on three of the fibers. One-standard deviation measurement spreads are 10, 18, and 26% as referred to the averaged measured 3-dB frequency.

Results from the N.A. comparisons are encouraging. The average of the standard deviations from measurements on five fibers is 2.0%. Measurements on fiber E gave the least spread, 0.9% for one standard deviation. For the measurements on fiber E all participant's error bars mutually overlap, and measurement spread is less than the precision claimed by most participants.

A complete analysis of the comparisons will be given and reasons for discrepancies addressed. In some instances the comparisons serve to document the usefulness of the procedures tested.

(Invited paper, 25 min)

1. G. T. Holmes, "Propagation Parameter Measurement of Optical Waveguides," Proc. Soc. Photo-Opt. Instrum. Eng. **224**.
2. A. H. Cherin and E. D. Head, "A Fiber Concatenation Experiment Using a Standardized Loss Measurement Method," to be published.
3. M. Erikstrud *et al.*, Opt. Quantum Electron. **11**, 517 (1979).
4. G. W. Day and G. E. Chamberlain, National Bureau of Standards Report NBSIR 79-1608 (May 1979).
5. A. H. Cherin and W. B. Garner, Laser Focus **16**, 60 (Aug. 1980).

TUK2 Power distribution of backward scattered radiation in optical fibers

B. COSTA, P. MORRA, and B. SORRO, CSELT, Via G. Reiss Romoli, 274-10148 Turin, Italy.

When using the backscattering technique[1] for attenuation measurements it is assumed that the loss coefficient of the backscattered radiation is equal to that of the forward-propagating beam. However, the backscattered radiation is scattered nearly uniformly over all angles, producing a modal distribution generally different from that of the direct beam. To evaluate the effect of this phenomenon, we investigated the properties of backscattered radiation. First the near-field distribution of backscattered power along the fiber length was measured by sampling the return waveform at different times corresponding to different positions; this allowed the modal evolution of the backward beam to be studied. In addition different launching conditions were used to correlate backscattered power distribution to the forward one. The measurements were performed by projecting an enlarged image of the fiber input end onto the plane of a small photodetector, which allowed scanning along a diameter. Due to the very low amount of energy available, a high sensitivity backscattering apparatus was developed, with a dynamic range in excess of 40 dB. The achievable spatial resolution was ~3 μm. Since both launching and detection conditions remain unchanged when temporal scanning is performed, high sensitivity to small changes in power distributions is obtained. The fiber used in the experiment is a graded-index type, 62.5-μm core diam, 0.21 N.A., 1.1-km length. The near-field distribution of the launched beam was measured, for different launching conditions, both near the input end and at the output end. The results indicate that the fiber has only a small amount of mode conversion. The near field of backscattered power was measured. A first remark concerns the fact that a large redistribution of power among all modes, even in the case of small angle excitation, occurs. This could be expected as a consequence of the isotropic scattering process. However, the redistribution is not complete, and backscattered modal volume seems to be dependent on the forward one. As regards the evolution of near-field along the fiber a small reduction of high-order modes occurs as a function of length. This is visible in the change of refractive-index dip depth and lowering of power at large radii. This confirms a small amount of mode conversion. In conclusion the proposed technique seems to have the potential to provide a better understanding of backscattering measurements. Moreover it can be proposed as a nondestructive way of studying modal evolution in optical fibers as a function of length. Measurements are being repeated using a cavity-dumped krypton-pumped dye laser capable of providing 100-W peak pulses; better control of launching conditions will facilitate interpretation of results. Quantitative data are obtained by using the technique exposed in Ref. 2, thus allowing a comparison with theoretical models and evaluation of inaccuracies due to differential mode attenuation effects. **(12 min)**

1. M. K. Barnoski and S. M. Jensen, Appl. Opt. **15**, 2112 (1976).
2. M. Calzavara, P. Di Vita, and U. Rossi, submitted to this Conference.

TUK3 Fiber diameter variations and their effect on backscatter loss measurements

A. J. CONDUIT, D. N. PAYNE, and A. H. HARTOG, University of Delaware, Electronics Department, Southampton S09 5NH, U. K.

In a recent publication[1] it was shown that the commonly observed features in the fiber local-attenuation plots obtained by the backscatter method are associated with fiber-diameter fluctuations. In particular, it was demonstrated that propagation through a contracting taper produced a reduction in attenuation, the tapered section on occasions having an apparent negative loss. Conversely, an expanding taper exhibits a positive loss of similar magnitude. Both these effects are the reverse of that which might be intuitively expected. Figure 1 shows the measured backscatter power and local attenuation for the two cases. We have now isolated the mechanism which causes these apparent anomalies and present here a theoretical and experimental explanation.

The model used for the calculation is shown in Fig. 2. We assume that the forward-propagating pulse only partially excites the fiber and thus is able to traverse either a weakly expanding or contracting taper without loss. On the other hand, the scattered light excites the fiber fully for propagation in the return direction. Consequently, for an expanding taper, backscattered light is lost by radiation on passing through the taper, since it appears contracting in the return direction. The power lost is in proportion to the decrease in fiber core area [curve (a), Fig. 2], and thus the local loss curve exhibits an increase in observed loss [curve (a), Fig. 3].

For a contracting taper the situation is more complex; in this case the light backscattered downstream of the taper excites modes of both the core and cladding, and together these return to the source. The cladding modes are preferentially attenuated, but for positions not too far downstream, a proportion is able to couple into the core at the taper, since it appears expanding in the reverse direction. Thus the fiber can be thought to have an increased capture cross section for scattered light returned from a position following the taper. This results in an increase in scatter return [Fig. 2, curve (b)] and an apparent reduction in attenuation in proportion to the increase in core area [Fig. 3, curve (b)]. Note that the magnitude of the loss feature is approximately equal, but opposite, for the two effects; hence measurements in opposite directions on a fiber with diameter fluctuations will show anticorrelated features.[1,2] In addition, for high values of cladding loss the calculation for a contracting taper shows an overshoot as a result of the attenuation of cladding power [Figs. 2 and 3, curves (c)]. We have observed this effect in some of the fibers tested.

To verify the theoretical predictions, experiments were performed on a fiber in which a single 75-m taper had been programmed during fiber drawing. The measured backscattered power for propagation in opposite directions seems to be in close agreement with the calculated curves of Fig. 2. Further verification was demonstrated by removing the silicone coating from the fiber by immersion in strong sulfuric acid. The scatter return obtained with the fiber still in the acid showed a profound effect; a sevenfold increase was observed in the region of the taper, presumably as a result of scattering of cladding modes at the fiber–acid interface. To eliminate this, the fiber was immersed in index-matching liquid. The negative loss-producing feature was then much reduced, although it was not found possible to remove it completely, emphasizing the persistance of the low-order cladding modes which contribute to the effect. As predicted, the result for propagation into an expanding taper was totally unaffected by cladding removal.

We conclude that (1) the anticorrelated features in backscatter loss curves are caused by diameter variations and can be predicted by a mechanism which in one direction results from loss of backscattered power and, in the other, a reciprocal effect involving coupling from cladding modes; (2) the cladding modes can have a marked effect even in the face of high values of cladding loss, since the modes involved are low-order and persistent; (3) the cladding modes are expected to contribute to backscatter loss measurements even in fibers with lossy coatings, as evidenced by our results for immersion in acid. **(12 min)**

1. A. J. Conduit, D. N. Payne, and A. H. Hartog, in *Technical Digest, Sixth ECOC, U. York, 1980,* pp. 152–154.
2. P. DiVita and V. Rossi, Opt Quantum Electron. **11**, 17 (1980).

TUK4 Statistics of backscattering in single-mode fiber

W. EICKHOFF and R. ULRICH, Technische Universität Hamburg-Harburg, 2100 Hamburg 90, Federal Republic of Germany.

Rayleigh backscattering in single-mode fibers is helpful in loss measurements by OTDR and OFDR but troublesome when causing feedback to a semiconductor laser or when interfering with the signal in interferometric sensors. We show that the backscattered fraction of power $Q = I_{scatt}/I_{input}$ may fluctuate strongly for even minute variations of optical frequency ω or ambient temperature T, pressure p, or strain ϵ, possibly imposing severe limitations on applications.

For a simplified explanation, we ignore attenuation and polarization effects. With a monochromatic source, the relative amplitude of the backscattered light, referred to the center $x = 0$ of a fiber extending from $x = -l$ to $x = +l$, is

$$A = \int_{-l}^{l} \sigma(x) \exp(2i\beta_0 x)dx.$$

The real function $\sigma(x)$ represents the weighted roughness of the refractive index, and β_0 is the propagation constant. Slow variations of β_0 by changing ω, T, p, ϵ are assumed to cause a time-linear sweep, $\beta(t) = \beta_0 + \dot{\beta}t$. Consequently, A fluctuates,

$$A(t) = \int_{-l}^{+l} s(x) \exp(2i\dot{\beta}xt)dx.$$

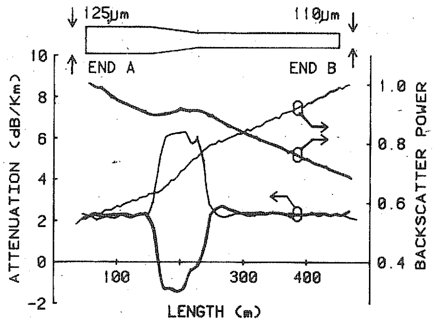

TUK3 Fig. 1. Backscatter measurements. Thick lines from end A, thin lines from end B.

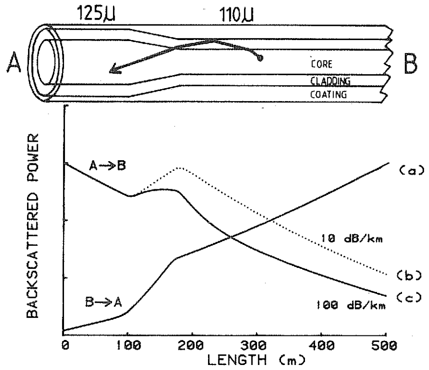

TUK3 Fig. 2. Calculated scatter return for directions shown and two values of cladding loss.

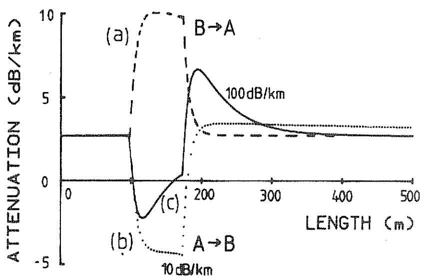

TUK3 Fig. 3. Local attenuation calculated from curves of Fig. 2.

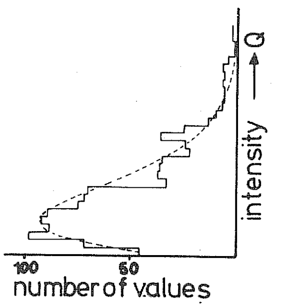

TUK4. Fig. 1. Histogram of time record of backscattered intensity showing statistical distribution.

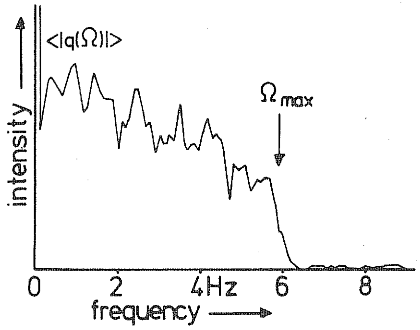

TUK4 Fig. 2. Average of twelve sets of data of frequency spectra.

The scattering function, $s(x) = \sigma(x)\exp(2i\beta_0 x)$, is a circular complex Gaussian random variable, and $A(t)$ is its band-limited Fourier transform, also having a Gaussian distribution. The intensity $Q(t) = |A(t)|^2$ fluctuates, therefore, with an exponential distribution of probability $P(Q) = \overline{Q}^{-1}\exp(-Q/\overline{Q})$ with mean value $\overline{Q}$, exactly like simple speckle patterns. Likewise, if a coherent background is superposed, the distribution changes to Rician.

Figure 1 is a histogram of 10^3 values of Q. The offset of the maximum from $Q = 0$ indicates the presence of a coherent background, resulting from spurious reflections. A Rician distribution (broken line) can be satisfactorily fitted. These data were obtained with a fiber of $2l = 17$ m, heated at 0.5°C/min, and a He–Ne laser.

The frequency spectrum of the fluctuating intensity

$$Q(t) = \int q(\Omega)\exp(i\Omega t)d\Omega,$$

has a ragged structure typical of the spectrum of a single time record $Q(t)$.

The average of twelve such spectra is smoother (Fig. 2). These spectra result from the mutual interferences of waves scattered by all possible combinations of path elements. In the absence of a coherent background, and with a monochromatic source, the noise power spectrum $|q(\Omega)|^2$ has a triangular shape. Its width Ω_{max} and height are both proportional to the fiber length, the total mean noise power $t^{-1}\int|q(\Omega)|^2 d\Omega$ equals the dc power $\overline{Q}^2$. The maximum noise frequency is $\Omega_{max} = 4l\dot{\beta}$. A frequency of 10 Hz obtains with a $2l$ = 100-m fiber, for example, when the temperature changes at a rate of 2.5×10^{-3} °C/sec, or the pressure at 2.5×10^{-2} bar/sec, or the longitudinal strain at 2.8×10^{-8} sec^{-1}, or the laser frequency at 100 MHz/sec. We shall discuss the reductions of noise resulting from attenuation and for less coherent sources.

(12 min)

TUK5 Measurement of cutoff wavelength and propagation curve in single-mode waveguides

V. A. BHAGAVATULA, Corning Glass Works, R&D Division, Corning, N.Y. 14830.

In the design and modeling of single-mode waveguides, one of the parameters of interest is the cutoff wavelength λ_c of the LP_{11} mode. In this paper we present measurements using an easily implemented refracted power technique which allows an accurate determination of this cutoff wavelength. The technique is based on the sudden change in refracted power at the cutoff wavelength, and the insensitivity to coating or leaky mode effects determines the intrinsic guide values. In addition this parameter, coupled with the transmitted power loss peaks induced by periodic curvature perturbations of a known frequency, allows the propagation constant β for the waveguide to be obtained. Such information is of interest in the design and microbend studies of single-mode waveguides.

The technique involves the measurement of the normalized refracted power as a function of wavelength.[1] The refracted power undergoes a sudden change at the LP_{11} mode cutoff, and from such data, the cutoff wavelength λ_c^R is determined. The experimental setup is shown in Fig. 1. The experimental details, the accuracy of the measurement, and a comparison with the cutoff wavelength determined by a transmitted power technique[2] will be presented.

Additionally, from a knowledge of the intrinsic guide cutoff wavelength λ_c^R and the transmission loss peaks due to periodic curvature perturbations at a known spatial frequency, the propagation curves for the LP_{11} and LP_{01} modes can be obtained. The periodic perturbation couples the bound power to the radiation modes according to the relation[3]

$$\beta - n_2 k = \frac{2\pi}{\Lambda}, \qquad (1)$$

where β is the propagation constant of the mode, k is the free space propagation number, and Λ is the wavelength of the periodic perturbation. The knowledge of

$$\Delta\beta_i = \frac{2\pi}{\Lambda_i} \text{ and } \Delta\lambda_i = \lambda_c^R - \lambda_i^P$$

allows the propagation curve to be plotted. The wavelengths of maximum coupling λ_i^P, indicated by the loss peaks in the normalized transmitted power, are shown in Fig. 2 for various perturbation frequencies.

The preliminary results indicate that the propagation constants for the fiber in Fig. 2 do not exactly satisfy the step-index values. The deviations can be due to nonstep index profiles, a higher frequency curvature perturbation, etc. Additional results to identify the source of this deviation and correlation with the fiber parameters and index profiles will be presented.

A new cutoff wavelength measurement technique based on refracted power is described for single-mode waveguides. This technique is easily implemented and being insensitive to external perturbations or leaky modes leads to the evaluation of intrinsic guide values. This may provide a suitable technique for standardizing the measurement of λ_c for single-mode waveguides. A procedure to obtain the propagation constant using this true cutoff value is illustrated. These results are of interest in the design and modeling studies of microbend losses in single-mode waveguides. **(12 min)**

1. V. A. Bhagavatula, W. F. Love, D. B. Keck, and R. A. Westwig, Electron. Lett. **16**, 695 (1980).
2. Y. Katsuyoma, M. Tokuda, N. Uchida, and M. Nakahara, Electron. Lett. **12**, 669 (1976).
3. D. Marcuse, Bell Syst. Tech. J. **55**, 937 (1976).

TUK6 Subpicosecond cinematographic display of modes of a fiber

A. BARTHELEMY, J. PIASECKI, and C. FROEHLY, Laboratoire d'Optique (ERA CNRS 535), F-87060 Limoges Cedex, France.

We describe a new coherent optics technique which selects each of the modes excited in meter-length samples of multimode fibers by discriminating the time of flight of the mode. The result of the observation reported is equivalent to subpicosecond sequential display of the output end of the fiber in which a short light pulse would have been injected.

This is achieved by coherent optical spectroscopy combining dye laser illumination, two-beam interferometry, and temporal frequency filtering in a two-stage spectroscope. Each mode of the fiber gives rise to a channeled spectrum, the spatial frequency of which encodes the mode temporal delay. The spectrogram resulting from the coherent superposition of all the excited modes is a generalized channeled spectrum, the Fourier components of which can be selected on a spatial frequency filtering bench.

After this filtering step, successive images of the excited modes will be singled out with simultaneous subpicosecond measurements of their times of flight.

Experimental results obtained with this technique on a fiber having several modes will be presented.

(12 min)

Tuesday **AFTERNOON**
28 April 1981 **TUL**
EMBARCADERO ROOM

3:45 PM **Coupling and Switches**

L. Dworkin, Presider

TUL1 High efficiency coupling from laser diodes into single-mode fibers with quadrangular pyramid-shaped hemielliptical ends

H. SAKAGUCHI, N. SEKI, and S. YAMAMOTO, KDD R&D Laboratories, 1-23, Nakameguro 2-chome, Meguro-ku, Tokyo 153, Japan.

To reduce the coupling loss between laser diodes and single-mode fibers (SMF), microlenses formed on fiber input ends by various methods have been reported.[1–6] Among these microlenses, the ones formed out of the fiber itself are solid and have stable optical properties. However, the conventional fabrication methods are limited to hemispherical or hemicylindrical microlenses, and the lenses are applicable only to specific stripe lasers. We propose a way of coupling fibers with quadrangular pyramid-shaped hemielliptical ends. This fabrication method enables SMFs to couple with any stripe laser by controlling the initial geometry of the pyramids. Theory shows that hemielliptical ends improve the losses by 0.5–2 dB compared with hemispherical ends with a 2–3-μm beam spot size in the junction plane.

Hemielliptical ends were fabricated as follows: After being polished into quadrangular pyramids with rectangular cross section, the fiber ends were melted in an arc discharge to form the desired shape. The ellipticity of the ends was determined by the initial cross section of the pyramids, and their radii of curvature were controlled by the discharge duration, current, and number of melts.

Laser diodes are InGaAsP lasers emitting at 1.3 or 1.5 μm. Beam spot sizes of laser diodes and corresponding SMF mode radii were estimated from far-field measurements. Experimental results of coupling for the hemielliptical-end and flat-end SMF are shown in Table I. Coupling losses of 2.87, 3.63, and 3.76 dB were achieved for laser diodes 1, 2, and 3, respectively. The relative loss dependence on fiber displacements from its optimum position, along directions parallel and perpendicular to the junction plane and along fiber axial direction, is illustrated in Fig. 1 for the coupling from laser diode 1 into SMF with the hemielliptical end. Permissible displacements for a 1-dB loss increase along these directions are 1.1, 0.9, and 7.0 μm, respectively. SMF outputs as a function of the axial separation between laser diode 1 and SMF are shown in Fig. 2 for the hemielliptical-end and flat-end SMF. The power oscillation with half wavelength periods implies a Fabry-Perot interference between the laser diode facet and fiber input plane. Comparing the power fluctuations at each optimum separation of coupling, the fluctuation for the hemielliptical end is about one tenth of that of the flat end. SMF with hemielliptical ends are less sensitive to reflected light than those with flat ends.

A high efficient coupling from laser diodes into single-mode fibers has been achieved by the pyramid-shaped hemielliptical ends. Low coupling losses of 2.87–3.76 dB were obtained for laser diodes with various kinds of stripe geometry. Further improvements are expected by optimizing the lens properties. **(12 min)**